Urine proteome changes in rats subcutaneously inoculated with approximately ten tumor cells

Jing Wei, Wenshu Meng and Youhe Gao

Department of Biochemistry and Molecular Biology, Beijing Normal University, Gene Engineering Drug and Biotechnology Beijing Key Laboratory, Beijing, China

ABSTRACT

Background. Biomarkers are changes associated with the disease. Urine is not subject to homeostatic control and therefore accumulates very early changes, making it an ideal biomarker source. Usually, we have performed urinary biomarker studies involving at least thousands of tumor cells. However, no tumor starts from a thousand tumor cells. We therefore examined urine proteome changes in rats subcutaneously inoculated with approximately ten tumor cells.

Methods. Here, we serially diluted Walker-256 carcinosarcoma cells to a concentration of 10^2/mL and subcutaneously inoculated 0.1 mL of these cells into nine rats. The urine proteomes on days 0, 13 and 21 were analyzed by liquid chromatography coupled with tandem mass spectrometry.

Results. Hierarchical clustering analysis showed that the urine proteome of each sample at three time points were clustered into three clusters, indicating the good consistency of these nine rats when inoculated with the same limited tumor cells. Differential proteins on days 13 and 21 were mainly associated with cell adhesion, autophagic cell death, changes in extracellular matrix organization, angiogenesis, and the pentose phosphate pathway. All of these enriched functional processes were reported to contribute to tumor progression and could not be enriched through random allocation analysis.

Conclusions. Our results indicated that (1) the urine proteome reflects changes associated with cancer even with only approximately ten tumor cells in the body and that (2) the urine proteome reflects pathophysiological changes in the body with extremely high sensitivity and provides potential for a very early screening process of clinical patients.

Subjects Animal Behavior, Biochemistry, Bioinformatics, Oncology

Keywords Urine, Biomarker, Sensitive resource, Proteomics

Submitted 20 May 2019
Accepted 21 August 2019
Published 17 September 2019

Corresponding author
Youhe Gao, gaoyouhe@bnu.edu.cn

Academic editor
Mohammed Gagaoua

Additional Information and Declarations can be found on page 13

DOI **10.7717/peerj.7717**

INTRODUCTION

Urine is an ideal biomarker resource. Blood often remains stable because of homeostatic mechanisms. However, as the filtrate of blood, urine has no need to remain stable and thus tolerates a much higher degree of changes. Therefore, urine can accumulate all changes from the whole body and may provide the potential to detect early and small changes in the body (*Gao, 2013*). Urine is easily affected by various physiological factors, such as sex, age and diet (*Wu & Gao, 2015*). In patients, the urine proteome is easily influenced by certain medications because of necessary therapeutic measures. Therefore, our laboratory

proposed a strategy for urinary biomarker studies. First, we used animal models to find early biomarkers of related diseases. Then, we verified candidate biomarkers in clinical urine samples (*Gao, 2014*). The use of animal models minimizes external influencing factors, such as diet, gender, age, medications and some environmental factors. In addition, using animal models will allow identification of the exact start of the disease, which is helpful in the early detection of cancer. Differential urinary proteins found in animal models are likely to be directly associated with related diseases. According to this strategy, our laboratory has applied different types of animal models, such as subcutaneous tumor-bearing model (*Wu, Guo & Gao, 2017a*), pulmonary fibrosis model (*Wu et al., 2017b*), glioma model (*Ni et al., 2018*), liver fibrosis model (*Zhang et al., 2018a*), Alzheimer's disease model (*Zhang et al., 2018b*), chronic pancreatitis model (*Zhang, Li & Gao, 2018c*) and myocarditis model (*Zhao et al., 2018*), to search for early biomarkers before pathological changes and clinical manifestations.

Urine can reflect changes more sensitively than blood. It has been reported that even when interference is introduced into the blood with two anticoagulants, changes in the abundance of more proteins were consistently detected in urine samples than in plasma (*Li, Zhao & Gao, 2014*). In addition, the urine proteome has been applied to detect tumors in various tumor-bearing animals. For example, (i) in W256 subcutaneously tumor-bearing rats, a total of ten differential urinary proteins were identified before a tumor mass was palpable (*Wu, Guo & Gao, 2017a*); (ii) in the intracerebral W256 tumor model, nine urinary proteins changed significantly before any obvious clinical manifestations or abnormal magnetic resonance imaging (MRI) signals (*Zhang et al., 2019*); (iii) in the glioma rat model, a total of thirty differential proteins were identified before MRI (*Ni et al., 2018a*); (iv) a total of seven urinary proteins changed in both lung tumor-bearing mice and lung cancer patients, indicating their potential roles in the early detection of lung cancer (*Zhang et al., 2015*); (v) in a urothelial carcinoma rat model, differential urinary proteins from upregulated biological processes might be seen as candidate biomarkers (*Ferreira et al., 2015*). All of these studies were performed involving thousands of tumor cells; however, no tumor starts from a thousand tumor cells. Since urine is a more sensitive biomarker resource than blood, we explored the sensitivity limit of urine. We determined whether the urine proteome changes if there are only a small number of tumor cells in the body.

In this study, we subcutaneously injected approximately ten Walker-256 carcinosarcoma cells into nine rats. Urine samples were collected on days 0, 13, and 21. Urine proteins were analyzed by liquid chromatography-tandem mass spectrometry (LC-MS/MS). Differential proteins on days 13 and 21 were analyzed by functional enrichment analysis to find associations with tumor progression. This research aimed to determine whether the urine proteome could reflect changes associated with these ten tumor cells. The technical flowchart is presented in Fig. 1.

MATERIAL AND METHODS

Animal treatment

Male Wistar rats ($n = 12$, 150 ± 20 g) were purchased from Beijing Vital River Laboratory Animal Technology Co., Ltd. Animals were maintained with a standard laboratory diet

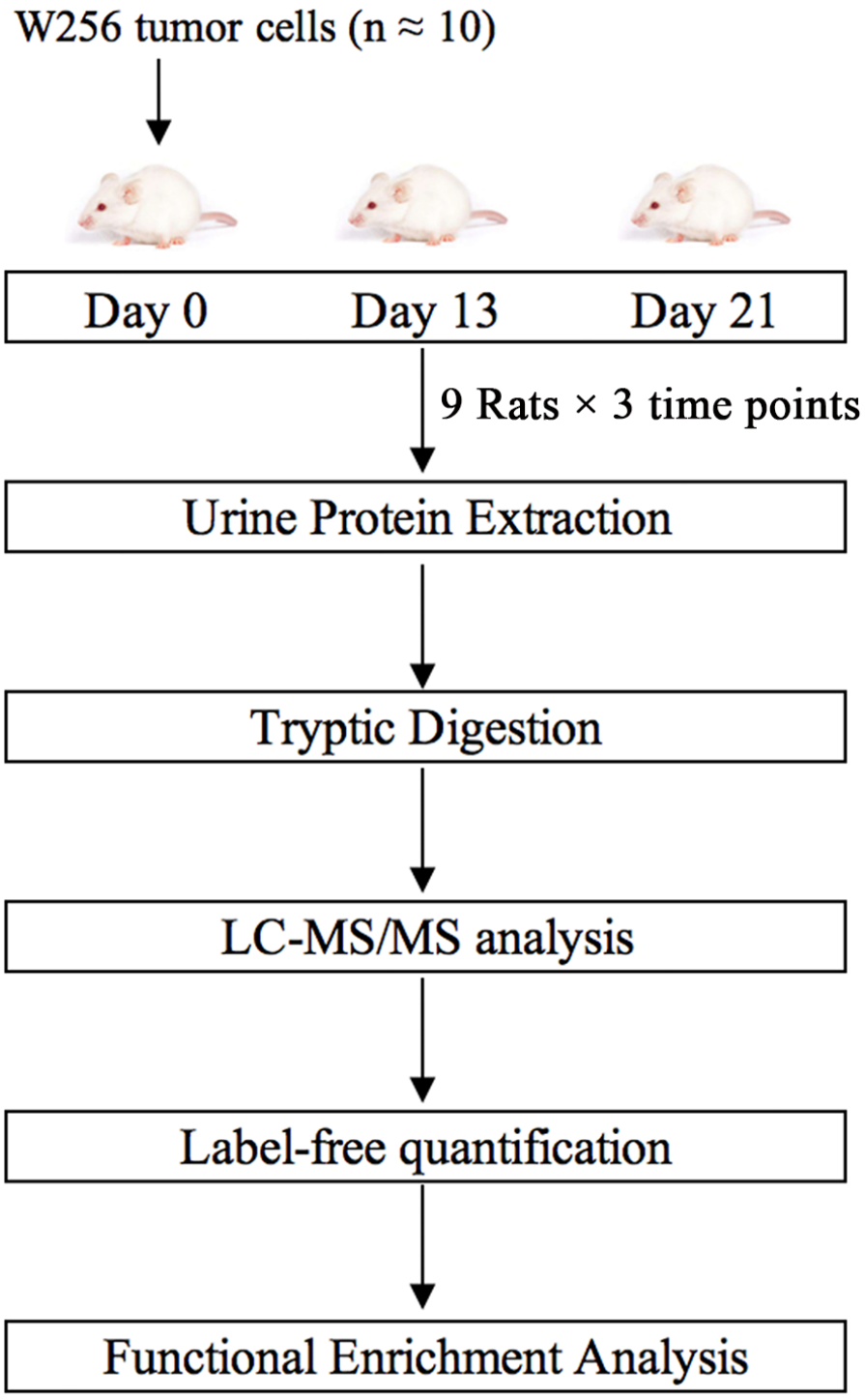

Figure 1 Workflow of protein identification in rats subcutaneously inoculated with ten tumor cells. Urine was collected on days 0, 13 and 21 after inoculation with tumor cells. Urinary proteins were extracted, digested, and identified by liquid chromatography coupled with tandem mass spectrometry (LC-MS/MS). Functional enrichment analysis of differential proteins was performed by DAVID and IPA.
Full-size DOI: 10.7717/peerj.7717/fig-1

under controlled indoor temperature (21 ± 2 °C), humidity (65–70%) and 12 h/12 h light–dark cycle conditions. The experiment was approved by Peking Union Medical College (Approval ID: ACUC-A02-2014-008).

Walker-256 (W256) carcinosarcoma cells were purchased from the Cell Culture Center of the Chinese Academy of Medical Sciences (Beijing, China). W256 tumor cells were intraperitoneally inoculated into Wistar rats. The W256 ascites tumor cells were harvested from the peritoneal cavity after seven days. After two cell passages, the W256 ascites tumor cells were collected, centrifuged, and resuspended in 0.9% normal saline (NS). Then, W256 tumor cells were serially diluted to a concentration of 10^2/mL. The viability of W256 cells was evaluated by the Trypan blue exclusion test using a Neubauer chamber, and only 95% viable tumor cells were used for serially dilution.

The rats were randomly divided into the following two groups: rats subcutaneously inoculated with tumor cells ($n = 9$) and control rats ($n = 3$). In the experimental group, rats were inoculated with 10 W256 cells in 100 μL of NS into the right flank of the rats. The control rats were subcutaneously inoculated with an equal volume of NS. All rats were anesthetized with sodium pentobarbital solution (four mg/kg) before inoculation.

Urine collection

Before urine collection, all rats were accommodated in metabolic cages for 2–3 days. Urine samples were collected from rats subcutaneously inoculated with tumor cells ($n = 9$) on days 0, 13 and 21. All rats were placed in metabolic cages individually for 12 h to collect urine without any treatment. After collection, urine samples were stored immediately at −80 °C.

Extraction and digestion of urinary proteins

Urine samples ($n = 27$) were centrifuged at 12,000 × g for 30 min at 4 °C. Then, the supernatants were precipitated with three times the volume of ethanol at −20 °C overnight. The pellets were dissolved sufficiently in lysis buffer (8 mol/L urea, 2 mol/L thiourea, 50 mmol/L Tris, and 25 mmol/L DTT). After centrifugation at 4 °C and 12,000 × g for 30 min, the protein samples were measured by using the Bradford assay. A total of 100 μg of each protein sample was digested with trypsin (Trypsin Gold, Mass Spec Grade, Promega, Fitchburg, WI, USA) by using filter-aided sample preparation (FASP) methods (*Wisniewski et al., 2009*). These digested peptides were desalted using Oasis HLB cartridges (Waters, Milford, MA, USA) and then dried by vacuum evaporation (Thermo Fisher Scientific, Bremen, Germany).

LC-MS/MS analysis

Digested peptides ($n = 27$) were dissolved in 0.1% formic acid to a concentration of 0.5 μg/μL. For analysis, one μg of peptide from each sample was loaded into a trap column (75 μm ×2 cm, three μm, C18, 100 Å) at a flow rate of 0.25 μL/min and then separated with a reversed-phase analytical column (75 μm ×250 mm, two μm, C18, 100 Å). Peptides were eluted with a gradient extending from 4%–35% buffer B (0.1% formic acid in 80% acetonitrile) for 90 min and then analyzed with an Orbitrap Fusion Lumos Tribrid Mass Spectrometer (Thermo Fisher Scientific, Waltham, MA, USA). The MS data were acquired

using the following parameters: (i) data-dependent MS/MS scans per full scan were auquired at the top-speed mode; (ii) MS scans had a resolution of 120,000, and MS/MS scans had a resolution of 30,000 in Orbitrap; (iii) HCD collision energy was set to 30%; (iv) dynamic exclusion was set to 30 s; (v) the charge-state screening was set to +2 to +7; and (vi) the maximum injection time was 45 ms. Each peptide sample was analyzed twice.

Label-free quantification

Raw data files ($n = 54$) were searched using Mascot software (version 2.5.1; Matrix Science, London, UK) against the Swiss-Prot rat database (released in February 2017, containing 7,992 sequences). The parent ion tolerance was set to 10 ppm, and the fragment ion mass tolerance was set to 0.02 Da. The carbamidomethylation of cysteine was set as a fixed modification, and the oxidation of methionine was considered a variable modification. Two missed trypsin cleavage sites were allowed, and the specificity of trypsin digestion was set for cleavage after lysine or arginine. Dat files ($n = 54$) were exported from Mascot software and then processed using Scaffold software (version 4.7.5, Proteome Software Inc., Portland, OR). The parameters were set as follows: both peptide and protein identifications were accepted at a false discovery rate (FDR) of less than 1.0% and proteins were identified with at least two unique peptides. Different samples were compared after normalization with the total spectra. Protein abundances at different time points were compared with spectral counting, according to previously described procedures (*Old et al., 2005*; *Schmidt et al., 2014*).

Statistical analysis

Average normalized spectral counts of each sample were used for the following statistical analysis. The levels of proteins identified on days 13 and 21 were compared with their levels on day 0. Differential proteins were selected with the following criteria: unique peptides ≥ 2; fold change ≥ 1.5 or ≤ 0.67; average spectral count in the high-abundance group ≥ 3; comparison between two groups were conducted using two-sided, unpaired t-test; and P-values of group differences were adjusted by the Benjamini and Hochberg method (*Benjamini & Hochberg, 1995*). Group differences resulting in adjusted P-values <0.05 were considered statistically significant. All results are expressed as the mean $\pm$ standard deviation.

Functional enrichment analysis

Differential proteins on days 13 and 21 were analyzed by Gene Ontology (GO) based on the biological process, cellular component and molecular function categories using the Database for Annotation, Visualization and Integrated Discovery (DAVID) (*Huang da, Sherman & Lempicki, 2009*). The biological pathway enrichment at the two time points was analyzed with IPA software (Ingenuity Systems, Mountain View, CA, USA).

RESULTS

Characterization of rats subcutaneously inoculated with tumor cells

A total of 12 male Wistar rats (150 $\pm$ 20 g) were randomly divided into the following two groups: a control group ($n = 3$) and a group of rats subcutaneously inoculated with W256

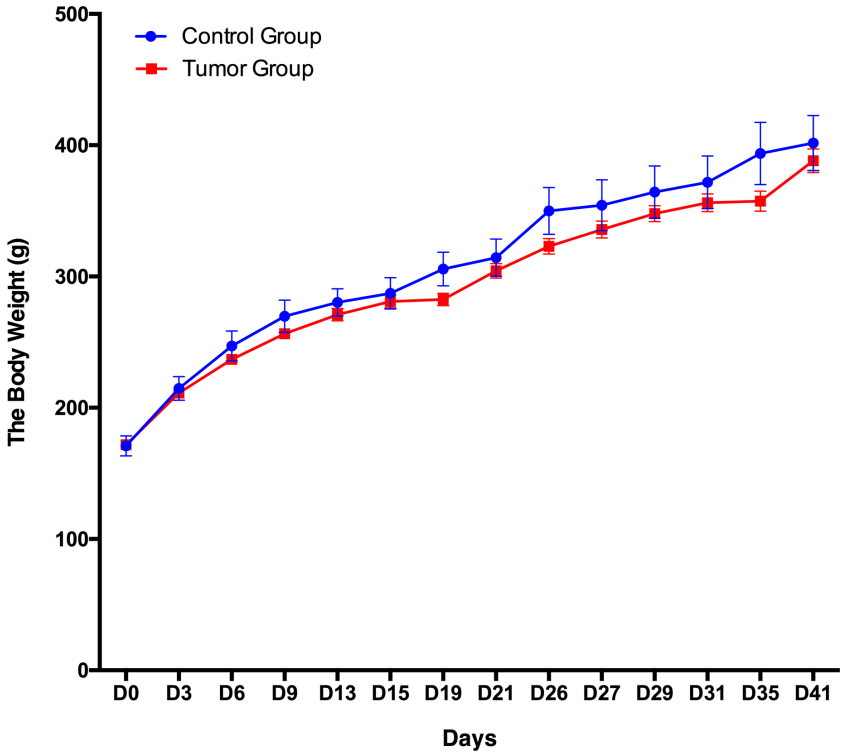

Figure 2 **Body weight changes between the rats subcutaneously inoculated with tumor cells and the control rats.**

Full-size DOI: 10.7717/peerj.7717/fig-2

tumor cells ($n = 9$). The body weight of these 12 rats was recorded every 3–5 days, and the daily behavior changes of the two groups were observed. The body weight of the group of rats subcutaneously inoculated with W256 tumor cells was slightly lower than that of the rats in the control group, but there were no significant differences until day 41 (Fig. 2). In addition, we did not observe any detectable tumor mass in the whole period. The rats in the control group performed normal daily activities and had shiny hair. There were no significant differences in daily behavior between these two groups.

Urine proteome changes

Twenty-seven urine samples at three time points (days 0, 13, and 21) were used for label-free LC-MS/MS quantitation. A total of 824 urinary proteins with at least 2 unique peptides were identified with <1% FDR at the protein level (Table S1). A hierarchical clustering was performed by using the complete linkage method. As shown in Fig. 3A, all technical replications within one sample were clustered together, indicating that the technical variation was smaller than the interindividual variation. In addition, all 824 proteins were clustered into three clusters, which almost corresponded to the urine proteome samples from the same group on day 0, day 13 and day 21 (except rat4-D0 and rat6-D21), indicating that intragroup technical variation was smaller than the intergroup biological variation and showed good consistency among these nine rats when inoculated with the same

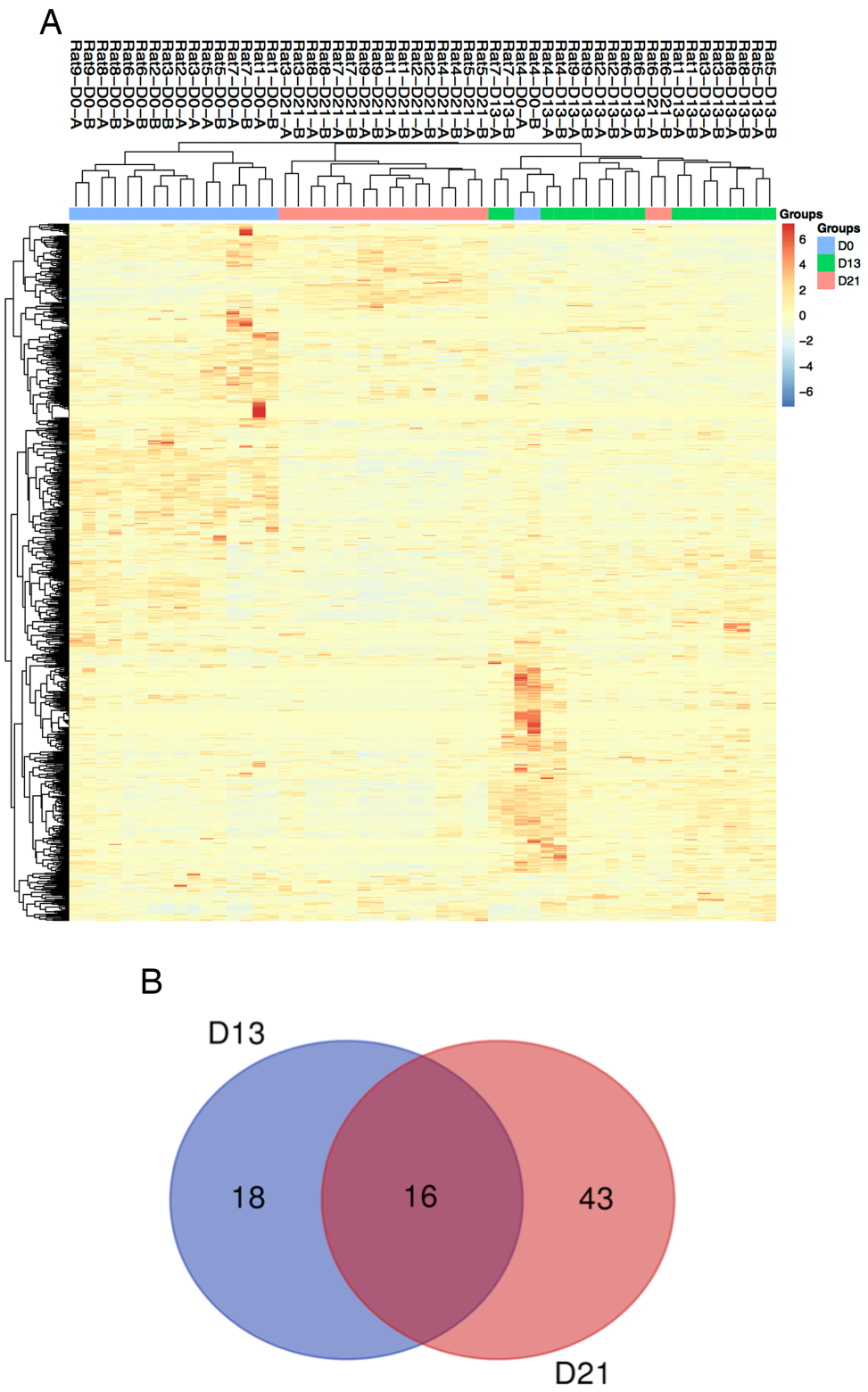

Figure 3 Proteomic analysis of urine samples on days 13 and 21 in rats subcutaneously inoculated with tumor cells. (A) Unsupervised cluster analysis of all proteins identified by LC-MS/MS. (B) Overlap evaluation of the differential proteins identified on days 13 and 21.

Full-size DOI: 10.7717/peerj.7717/fig-3

limited number of tumor cells. Using screening criteria, 34 and 59 differential proteins were identified on days 13 and 21, respectively. The overlap of these differential proteins is shown by a Venn diagram in Fig. 3B. Details are presented in Table 1.

Functional analysis

Functional enrichment analysis of differential proteins was performed by DAVID (*Huang da, Sherman & Lempicki, 2009*). Differential proteins were classified into biological processes, cellular components and molecular functions. The major biological pathways of differential proteins were enriched by IPA software. A significance threshold of $P < 0.05$ was used in all these representative lists.

Lists of fourteen representative biological processes on days 13 and 21 are presented in Fig. 4A. Cell adhesion, negative regulation of endopeptidase activity and organ regeneration were overrepresented both on days 13 and 21. Blood coagulation, acute-phase response, autophagic cell death, positive regulation of cell proliferation, extracellular matrix organization, and response to glucose were independently overrepresented on day 13. On day 21, heterophilic cell–cell adhesion via plasma membrane cell adhesion molecules, proteolysis, positive regulation of phagocytosis and angiogenesis were independently enriched.

To identify the biological pathways involved with the differential urine proteins, IPA software was used for canonical pathway enrichment analysis. A total of 18 and 13 significant pathways were enriched on days 13 and 21, respectively (Fig. 4B). Among these pathways, enriched intrinsic prothrombin activation pathway, coagulation system, acute phase response signaling, extrinsic prothrombin activation pathway and NAD phosphorylation and dephosphorylation were overrepresented on days 13 and 21. In addition, some representative pathways, such as autophagy, phagosome maturation and the role of tissue factor in cancer, were independently enriched on day 13, and the complement system was enriched only on day 21.

The enriched cellular components and molecular functions are presented in Fig. S1. The majority of differential proteins were derived from the extracellular exosomes, extracellular space and extracellular matrix (Fig. S1A). In the molecular function category, serine-type endopeptidase inhibitor activity and calcium ion binding were overrepresented on both on days 13 and 21 (Fig. S1B).

Random allocation statistical analysis

To confirm that these differential proteins on days 13 and 21 were indeed due to the ten subcutaneously inoculated W256 tumor cells, we randomly allocated the data of these 27 samples (Number 1 to Number 27) into three groups. We tried three random allocations, and the numbers in these three groups are shown in Table 2. In each iteration, we used the data of group 1 as the control group. When we used the previous criteria to screen differential urinary proteins, it was found that the adjusted *P*-values value on days 13 and 21 were all >0.05. No differential proteins were selected in these three randomly allocated trials. Details are shown in Tables S2, S3 and S4.

Table 1 Differentially proteins identified on day 13 and day 21.

Uniprot ID	Human ortholog	Description	Trends	ANOVA *P*-value	Average fold change	
					Day 13	Day 21
P02761	NO	Cluster of Major urinary protein	↑	<0.00010	4.70	7.59
P06760	P08236	Beta-glucuronidase	↑	0.0073	3.56	4.55
Q9JI85	P80303	Nucleobindin-2	↑	0.00018	2.74	3.69
P27590	P07911	Uromodulin	↑	<0.00010	2.31	2.65
P97603	Q92859	Neogenin (Fragment)	↓	<0.00010	0.43	0.21
P20611	P11117	Lysosomal acid phosphatase	↓	<0.00010	0.56	0.46
Q9ESS6	P50895	Basal cell adhesion molecule	↓	<0.00010	0.56	0.40
Q63556	NO	Serine protease inhibitor A3M (Fragment)	↓	<0.00010	0.47	0.48
O35112	Q13740	CD166 antigen	↓	<0.00010	0.41	0.33
Q63416	Q06033	Inter-alpha-trypsin inhibitor heavy chain H3	↓	<0.00010	0.32	0.23
O70535	P42702	Leukemia inhibitory factor receptor	↓	<0.00010	0.29	0.35
P13596	P13591	Neural cell adhesion molecule 1	↓	<0.00010	0.28	0.36
P35444	P49747	Cartilage oligomeric matrix protein	↓	<0.00010	0.27	0.42
P07897	P16112	Aggrecan core protein	↓	<0.00010	0.23	0.30
P26453	P35613	Basigin	↓	0.00094	0.23	0.21
Q9EPF2	P43121	Cell surface glycoprotein MUC18	↓	<0.00010	0.18	0.08
P38918	O95154	Aflatoxin B1 aldehyde reductase member 3	↑	0.0028	3.36	–
Q63530	Q96BW5	Phosphotriesterase-related protein	↑	0.0004	3.18	–
P24268	P07339	Cathepsin D	↑	<0.00010	1.56	–
P18292	P00734	Prothrombin	↓	<0.00010	0.60	–
P04937	P02751	Fibronectin	↓	<0.00010	0.61	–
P08592	NO	Amyloid beta A4 protein	↓	<0.00010	0.56	–
Q91XN4	Q13145	BMP and activin membrane-bound inhibitor homolog	↓	0.003	0.55	–
Q9JLS4	Q6FHJ7	Secreted frizzled-related protein 4	↓	0.00053	0.52	–
Q63467	P04155	Trefoil factor 1	↓	0.00026	0.50	–
Q62930	P02748	Complement component C9	↓	0.0055	0.49	–
P24090	P02765	Alpha-2-HS-glycoprotein	↓	0.00026	0.47	–
P97546	Q9Y639	Neuroplastin	↓	<0.00010	0.47	–
P26644	P02749	Beta-2-glycoprotein 1	↓	0.00016	0.46	–
Q5HZW5	Q9NPF0	CD320 antigen	↓	<0.00010	0.45	–
Q8JZQ0	P09603	Macrophage colony-stimulating factor 1	↓	0.00013	0.42	–
P07154	P07711	Cathepsin L1	↓	0.00021	0.40	–
D3ZTE0	P00748	Coagulation factor XII	↓	<0.00010	0.25	–
P07171	P05937	Cluster of Calbindin	↓	<0.00010	0.05	–
Q63475	Q92932	Receptor-type tyrosine-protein phosphatase N2	↓	<0.00010	–	6.25
P00714	P00709	Alpha-lactalbumin	↑	<0.00010	–	3.77
Q05175	P80723	Brain acid soluble protein 1	↑	<0.00010	–	3.69
Q4V885	Q5KU26	Collectin-12	↑	0.0011	–	2.28
O55004	P34096	Ribonuclease 4	↑	0.00023	–	2.13

(*continued on next page*)

Table 1 (*continued*)

Uniprot ID	Human ortholog	Description	Trends	ANOVA *P*-value	Average fold change	
					Day 13	Day 21
P81828	NO	Urinary protein 2	↑	<0.00010	–	1.96
P62986	P62987	Ubiquitin-60S ribosomal protein L40	↑	0.0011	–	1.81
P36374	NO	Prostatic glandular kallikrein-6	↑	0.0034	–	1.78
P80202	P36896	Activin receptor type-1B	↑	<0.00010	–	1.76
P06866	P00739	Haptoglobin	↑	0.00036	–	1.68
P07151	P61769	Beta-2-microglobulin	↑	<0.00010	–	1.65
P08937	NO	Odorant-binding protein	↑	0.002	–	1.51
P05544	NO	Serine protease inhibitor A3L	↓	0.00026	–	0.64
P29598	P00749	Urokinase-type plasminogen activator	↓	<0.00010	–	0.62
P05545	NO	Serine protease inhibitor A3K	↓	<0.00010	–	0.61
Q01460	Q01459	Di-N-acetylchitobiase	↓	<0.00010	–	0.61
Q642A7	Q8WW52	Protein FAM151A	↓	0.00045	–	0.58
P21704	P24855	Deoxyribonuclease-1	↓	<0.00010	–	0.56
P63018	P11142	Cluster of Heat shock cognate 71 kDa protein	↓	0.00045	–	0.56
P61972	P61970	Nuclear transport factor 2	↓	0.0024	–	0.54
Q68FQ2	Q9BX67	Junctional adhesion molecule C	↓	0.0011	–	0.53
P31211	P08185	Corticosteroid-binding globulin	↓	0.00011	–	0.48
Q9R0T4	P12830	Cadherin-1	↓	<0.00010	–	0.47
Q562C9	Q9BV57	1,2-dihydroxy-3-keto-5-methylthiopentene dioxygenase	↓	0.0057	–	0.43
O88917	NO	Adhesion G protein-coupled receptor L1	↓	<0.00010	–	0.42
Q9WUW3	P05156	Complement factor I	↓	<0.00010	–	0.42
P01026	P01024	Complement C3	↓	0.0071	–	0.42
P85971	O95336	6-phosphogluconolactonase	↓	0.0005	–	0.39
Q63751	NO	Vomeromodulin (Fragment)	↓	0.012	–	0.31
Q9EQV6	O14773	Tripeptidyl-peptidase 1	↓	0.0033	–	0.30
P53813	P07225	Vitamin K-dependent protein S	↓	0.00096	–	0.29
Q00657	Q6UVK1	Chondroitin sulfate proteoglycan 4	↓	<0.00010	–	0.28
P04073	P20142	Gastricsin	↓	0.00044	–	0.27
O70244	O60494	Cubilin	↓	<0.00010	–	0.25
Q1WIM1	Q8NFZ8	Cell adhesion molecule 4	↓	<0.00010	–	0.24
Q5I0D5	Q9H008	Phospholysine phosphohistidine inorganic pyrophosphate phosphatase	↓	<0.00010	–	0.20
Q63678	P25311	Zinc-alpha-2-glycoprotein	↓	<0.00010	–	0.20
Q99PW3	Q99519	Sialidase-1	↓	0.00025	–	0.18
Q641Z7	Q92484	Acid sphingomyelinase-like phosphodiesterase 3a	↓	<0.00010	–	0.18
P04785	P07237	Protein disulfide-isomerase	↓	<0.00010	–	0.17
Q6AYE5	Q86UD1	Out at first protein homolog	↓	<0.00010	–	0.16
P47820	P12821	Angiotensin-converting enzyme	↓	0.0016	–	0.13
Q80WD1	Q86UN3	Reticulon-4 receptor-like 2	↓	0.017	–	0.04

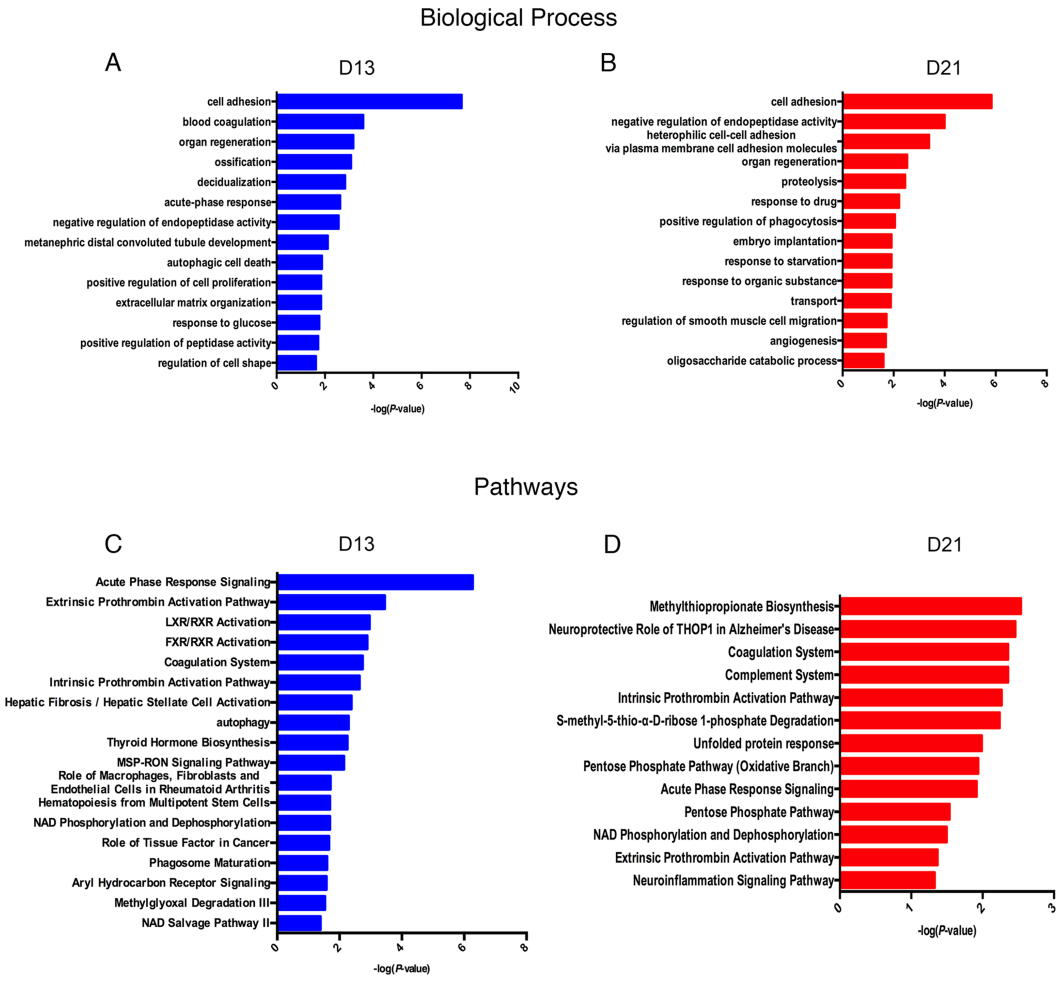

Figure 4 Functional analysis of differential proteins on days 13 and 21. (A) Dynamic changes in biological processes on day 13. (B) Dynamic changes in biological processes on day 21. (C) Dynamic changes in pathways on day 13. (D) Dynamic changes in pathways on day 21.

Full-size DOI: 10.7717/peerj.7717/fig-4

Table 2 Random allocation of the twenty-seven urine samples.

Randomly allocated	Group 1	Group 2	Group 3	Adjusted *P*-value
1	1, 4, 5, 12, 13, 14, 19, 20, 21	2, 3, 7, 11, 15, 17, 18, 22, 23	6, 8, 9, 10, 16, 24, 25, 26, 27	NO
2	1, 2, 3, 12, 13, 15, 25, 26, 27	4, 5, 6, 10, 11, 14, 19, 20, 21	7, 8, 9, 16, 17, 18, 22, 23, 24	NO
3	1, 7, 9, 11, 13, 16, 19, 21, 22	3, 4, 5, 10, 17, 18, 20, 25, 26	2, 6, 8, 12, 14, 15, 23, 24, 27	NO

Notes.

Numbers 1–9 represent Rat 1-D0 to Rat 9-D0; Numbers 10–18 represent Rat 1-D13 to Rat 9-D13; Numbers 19–27 represent Rat 1-D21 to Rat 9-D21.

DISCUSSION

Urine is an early and sensitive biomarker source that has been used for the early detection of cancer either in both animal models or clinical patients (*Beretov et al., 2015*; *Wu, Guo & Gao, 2017a*). However, no tumor starts from thousands of tumor cells. In this study, we subcutaneously inoculated approximately ten tumor cells into each of nine rats.

Unsupervised clustering analysis showed the good consistency after inoculation. A total of 34 and 59 differential proteins identified on days 13 and 21, respectively, and no urinary proteins changed after random allocation analysis.

After the functional enrichment analysis, we found that some enriched biological processes were reported to be associated with tumor progression. For example, (i) cell adhesion was usually reported to show a reduced number of tumor cells since 1962 (*Holmberg, 1962*); (ii) autophagic cell death occurs via the activation of autophagy, which has been reported to play roles in tumor suppression (*Mathew et al., 2009*); (iii) the positive regulation of cell proliferation is a common characteristic of cancer, and the inhibition of cancer cell proliferation may serve as a potential target for cancer treatment (*He et al., 2018*); (iv) changes in extracellular matrix organization were reported with crucial roles in cancer metastasis (*Goreczny et al., 2017*; *Sada et al., 2016*); (v) positive regulation of blood coagulation was frequently reported in cancer progression (*Tikhomirova et al., 2016*); and (vi) angiogenesis is still considered a common characteristic of tumorigenesis in many studies (*Baltrunaite et al., 2017*; *Protopsaltis et al., 2019*; *Ziegler et al., 2016*).

In addition, we found that some pathways were reported to play important roles in cancer. For example, (i) autophagy was reported to inhibit tumor progression (*Peng et al., 2016*); (ii) the MSP-RON signaling pathway was reported to play important roles in epithelial tumorigenesis (*Ma et al., 2010*) and will facilitate metastasis in prostate cancer cells (*Yin et al., 2017*); (iii) tissue factor (TF) expressed by tumor cells was reported to facilitate lung tumor progression (*Han et al., 2017*); (iv) upregulation of the pentose phosphate pathway (PPP) has been reported in several types of cancer (*Rao et al., 2015*); and (v) the enriched complement system pathway was reported to enhance the metastatic process of ovarian cancer cells (*Cho et al., 2016*). Our results indicated that even when limited tumor cells are present in the body, the urine proteome can reflect changes associated with cancer.

When comparing differential proteins identified in our research to W256 subcutaneously tumor-bearing model (*Wu, Guo & Gao, 2017a*) and intracerebral W256 tumor model (*Zhang et al., 2019*), we found that the proportion of overlapping proteins was small, and more than half of the differential proteins in each of the three tumor models were unique (Fig. S2). Comparing the differential proteins of the model inoculated with ten W256 cells and the W256 subcutaneously tumor-bearing model showed 25 overlapping proteins. We hypothesized that these small overlapping proteins may be due to the very different numbers of W256 tumor cells in these two animal models. Upon comparing the differences in the urine proteome between the ten tumor cell inoculated model and the intracerebral W256 tumor model, only 16 differential proteins overlapped, indicating that differential proteins were very different when the same tumor cells existed in different body parts. We also suppose that these proteomic profiles were different because the changes observed in this study were related to the very early phase of the tumor. Despite the small proportion of overlapping proteins, we found that cell adhesion was enriched in GO biological process analysis using either the 25 or 16 common differential proteins. This reduction in cell adhesion is a common characteristic of tumor cells (*Cavallaro & Christofori, 2001*). These

results suggest that although the tumor cell number and location differ, using limited tumor cells has the potential to simulate the early phase of tumor development.

Notably, it was difficult to ensure that exactly ten tumor cells were subcutaneously inoculated into each of nine rats. Given the limited number of animals in this preliminary study, a larger number of animals should be considered in future studies.

CONCLUSIONS

In this study, we aimed to observe changes in the urine proteome when inoculating approximately ten tumor cells into nine rats. Our results indicated that (1) the urine proteome reflects changes associated with cancer, even with a limited number of tumor cells in the body, and (2) the urine proteome reflects pathophysiological changes in the body with extremely high sensitivity, providing the potential for a very early screening process in clinical patients.

ADDITIONAL INFORMATION AND DECLARATIONS

Funding

This work was supported by the National Key Research and Development Program of China (2018YFC0910202 and 2016YFC1306300), the Beijing Natural Science Foundation (7172076), the Beijing Cooperative Construction Project (110651103), the Beijing Normal University (11100704), and the Peking Union Medical College Hospital (2016-2.27). The funders had no role in study design, data collection and analysis, decision to publish, or preparation of the manuscript.

Grant Disclosures

The following grant information was disclosed by the authors:
National Key Research and Development Program of China: 2018YFC0910202, 2016YFC1306300.
Beijing Natural Science Foundation: 7172076.
Beijing Cooperative Construction Project: 110651103.
Beijing Normal University: 11100704.
Union Medical College Hospital: 2016-2.27.

Competing Interests

The authors declare there are no competing interests.

Author Contributions

- Jing Wei conceived and designed the experiments, performed the experiments, analyzed the data, contributed reagents/materials/analysis tools, prepared figures and/or tables, authored or reviewed drafts of the paper, approved the final draft.
- Wenshu Meng performed the experiments, contributed reagents/materials/analysis tools.
- Youhe Gao conceived and designed the experiments, contributed reagents/materials/-analysis tools, authored or reviewed drafts of the paper, approved the final draft.

Animal Ethics

The following information was supplied relating to ethical approvals (i.e., approving body and any reference numbers):

The experiment was approved by Peking Union Medical College (Approval ID: ACUC-A02-2014-008).

Data Availability

The following information was supplied regarding data availability:

The data is available at figshare: Wei, Jing; Gao, Youhe (2019): Urine proteome changes in rats subcutaneously inoculated with approximately ten tumor cells. figshare. Dataset. https://figshare.com/articles/Urine_proteome_changes_in_rats_subcutaneously_inoculated_with_approximately_ten_tumor_cells_/9221084.

Supplemental Information

Supplemental information for this article can be found online at http://dx.doi.org/10.7717/peerj.7717#supplemental-information.

REFERENCES

Baltrunaite K, Craig MP, Palencia Desai S, Chaturvedi P, Pandey RN, Hegde RS, Sumanas S. 2017. ETS transcription factors Etv2 and Fli1b are required for tumor angiogenesis. *Angiogenesis* **20**:307–323 DOI 10.1007/s10456-017-9539-8.

Benjamini Y, Hochberg Y. 1995. Controlling the false discovery rate: a practical and powerful approach to multiple testing. *Journal of the Royal Statistical Society Series B* **57**:289–300.

Beretov J, Wasinger VC, Millar EK, Schwartz P, Graham PH, Li Y. 2015. Proteomic analysis of urine to identify breast cancer biomarker candidates using a label-free LC-MS/MS approach. *PLOS ONE* **10(11)**:e0141876 DOI 10.1371/journal.pone.0141876.

Cavallaro U, Christofori G. 2001. Cell adhesion in tumor invasion and metastasis: loss of the glue is not enough. *Biochimica Et Biophysica Acta* **1552**:39–45 DOI 10.1016/S0304-419X(01)00038-5.

Cho MS, Rupaimoole R, Choi HJ, Noh K, Chen J, Hu Q, Sood AK, Afshar-Kharghan V. 2016. Complement component 3 is regulated by TWIST1 and mediates epithelial-mesenchymal transition. *Journal of Immunology* **196**:1412–1418 DOI 10.4049/jimmunol.1501886.

Ferreira R, Oliveira P, Martins T, Magalhaes S, Trindade F, Pires MJ, Colaco B, Barros A, Santos L, Amado F, Vitorino R. 2015. Comparative proteomic analyses of urine from rat urothelial carcinoma chemically induced by exposure to N-butyl-N-(4-hydroxybutyl)-nitrosamine. *Molecular BioSystems* **11**:1594–1602 DOI 10.1039/c4mb00606b.

Gao Y. 2013. Urine-an untapped goldmine for biomarker discovery? *Science China Life Science* **56**:1145–1146 DOI 10.1007/s11427-013-4574-1.

Gao Y. 2014. Roadmap to the urine biomarker era. *MOJ Proteomics Bioinformatics* **1(1)**:18 DOI 10.15406/mojpb.2014.01.00005.

Goreczny GJ, Ouderkirk-Pecone JL, Olson EC, Krendel M, Turner CE. 2017. Hic-5 remodeling of the stromal matrix promotes breast tumor progression. *Oncogene* **36**:2693–2703 DOI 10.1038/onc.2016.422.

Han X, Zha H, Yang F, Guo B, Zhu B. 2017. Tumor-derived tissue factor aberrantly activates complement and facilitates lung tumor progression via recruitment of myeloid-derived suppressor cells. *International Journal of Molecular Science* **18(1)**:22 DOI 10.3390/ijms18010022.

He J, Chen Y, Cai L, Li Z, Guo X. 2018. UBAP2L silencing inhibits cell proliferation and G2/M phase transition in breast cancer. *Breast Cancer* **25**:224–232 DOI 10.1007/s12282-017-0820-x.

Holmberg B. 1962. Inhibition of cellular adhesion and pseudopodia formation by a dialysable factor from tumour fluids. *Nature* **195**:45–47 DOI 10.1038/195045a0.

Huang da W, Sherman BT, Lempicki RA. 2009. Systematic and integrative analysis of large gene lists using DAVID bioinformatics resources. *Nature Protocols* **4**:44–57 DOI 10.1038/nprot.2008.211.

Li M, Zhao M, Gao Y. 2014. Changes of proteins induced by anticoagulants can be more sensitively detected in urine than in plasma. *Science China Life Science* **57**:649–656 DOI 10.1007/s11427-014-4661-y.

Ma Q, Zhang K, Yao HP, Zhou YQ, Padhye S, Wang MH. 2010. Inhibition of MSP-RON signaling pathway in cancer cells by a novel soluble form of RON comprising the entire sema sequence. *International Journal of Oncology* **36**:1551–1561 DOI 10.3892/ijo_00000642.

Mathew R, Karp CM, Beaudoin B, Vuong N, Chen G, Chen HY, Bray K, Reddy A, Bhanot G, Gelinas C, Dipaola RS, Karantza-Wadsworth V, White E. 2009. Autophagy suppresses tumorigenesis through elimination of p62. *Cell* **137**:1062–1075 DOI 10.1016/j.cell.2009.03.048.

Ni Y, Zhang F, An M, Yin W, Gao Y. 2018. Early candidate biomarkers found from urine of glioblastoma multiforme rat before changes in MRI. *Science China Life Science* **61**:982–987 DOI 10.1007/s11427-017-9201-0.

Old WM, Meyer-Arendt K, Aveline-Wolf L, Pierce KG, Mendoza A, Sevinsky JR, Resing KA, Ahn NG. 2005. Comparison of label-free methods for quantifying human proteins by shotgun proteomics. *Molecularl & Cellular Proteomics* **4**:1487–1502 DOI 10.1074/mcp.M500084-MCP200.

Peng Y, Miao H, Wu S, Yang W, Zhang Y, Xie G, Xie X, Li J, Shi C, Ye L, Sun W, Wang L, Liang H, Ou J. 2016. ABHD5 interacts with BECN1 to regulate autophagy and tumorigenesis of colon cancer independent of PNPLA2. *Autophagy* **12**:2167–2182 DOI 10.1080/15548627.2016.1217380.

Protopsaltis NJ, Liang W, Nudleman E, Ferrara N. 2019. Interleukin-22 promotes tumor angiogenesis. *Angiogenesis* **22**:311–323 DOI 10.1007/s10456-018-9658-x.

Rao X, Duan X, Mao W, Li X, Li Z, Li Q, Zheng Z, Xu H, Chen M, Wang PG, Wang Y, Shen B, Yi W. 2015. O-GlcNAcylation of G6PD promotes the pentose phosphate pathway and tumor growth. *Nature Communications* **6**:1–10 DOI 10.1038/ncomms9468.

Sada M, Ohuchida K, Horioka K, Okumura T, Moriyama T, Miyasaka Y, Ohtsuka T, Mizumoto K, Oda Y, Nakamura M. 2016. Hypoxic stellate cells of pancreatic cancer stroma regulate extracellular matrix fiber organization and cancer cell motility. *Cancer Letters* **372**:210–218 DOI 10.1016/j.canlet.2016.01.016.

Schmidt C, Gronborg M, Deckert J, Bessonov S, Conrad T, Luhrmann R, Urlaub H. 2014. Mass spectrometry-based relative quantification of proteins in precatalytic and catalytically active spliceosomes by metabolic labeling (SILAC), chemical labeling (iTRAQ), and label-free spectral count. *RNA* **20**:406–420 DOI 10.1261/rna.041244.113.

Tikhomirova I, Petrochenko E, Malysheva Y, Ryabov M, Kislov N. 2016. Interrelation of blood coagulation and hemorheology in cancer. *Clinical Hemorheology and Microcirculation* **64**:635–644 DOI 10.3233/ch-168037.

Wisniewski JR, Zougman A, Nagaraj N, Mann M. 2009. Universal sample preparation method for proteome analysis. *Nature Methods* **6**:359–362 DOI 10.1038/nmeth.1322.

Wu J, Gao Y. 2015. Physiological conditions can be reflected in human urine proteome and metabolome. *Expert Review of Proteomics* **12**:623–636 DOI 10.1586/14789450.2015.1094380.

Wu J, Guo Z, Gao Y. 2017a. Dynamic changes of urine proteome in a Walker 256 tumor-bearing rat model. *Cancer Medicine* **6**:2713–2722 DOI 10.1002/cam4.1225.

Wu J, Li X, Zhao M, Huang H, Sun W, Gao Y. 2017b. Early detection of urinary proteome biomarkers for effective early treatment of pulmonary fibrosis in a rat model. *Proteomics Clinical Applications* **11**:11–12 DOI 10.1002/prca.201700103.

Yin B, Liu Z, Wang Y, Wang X, Liu W, Yu P, Duan X, Liu C, Chen Y, Zhang Y, Pan X, Yao H, Liao Z, Tao Z. 2017. RON and c-Met facilitate metastasis through the ERK signaling pathway in prostate cancer cells. *Oncology Reports* **37**:3209–3218 DOI 10.3892/or.2017.5585.

Zhang F, Ni Y, Yuan Y, Yin W, Gao Y. 2018a. Early urinary candidate biomarker discovery in a rat thioacetamide-induced liver fibrosis model. *Science China Life Science* **61**:1369–1381 DOI 10.1007/s11427-017-9268-y.

Zhang F, Wei J, Li X, Ma C, Gao Y. 2018b. Early candidate urine biomarkers for detecting alzheimer's disease before amyloid-beta plaque deposition in an APP (swe)/PSEN1dE9 transgenic mouse model. *Journal of Alzheimer's Disease* **66**:613–637 DOI 10.3233/jad-180412.

Zhang H, Cao J, Li L, Liu Y, Zhao H, Li N, Li B, Zhang A, Huang H, Chen S, Dong M, Yu L, Zhang J, Chen L. 2015. Identification of urine protein biomarkers with the potential for early detection of lung cancer. *Scientific Reports* **5**:11805 DOI 10.1038/srep11805.

Zhang L, Li Y, Gao Y. 2018c. Early changes in the urine proteome in a diethyldithiocarbamate-induced chronic pancreatitis rat model. *Journal of Proteomics* **186**:8–14 DOI 10.1016/j.jprot.2018.07.015.

Zhang L, Li Y, Meng W, Ni Y, Gao Y. 2019. Dynamic urinary proteomic analysis in a Walker 256 intracerebral tumor model. *Cancer Medicine* **8**:3553–3565 DOI 10.1002/cam4.2240.

Zhao M, Wu J, Li X, Gao Y. 2018. Urinary candidate biomarkers in an experimental autoimmune myocarditis rat model. *Journal of Proteomics* **179**:71–79 DOI 10.1016/j.jprot.2018.02.032.

Ziegler ME, Hatch MM, Wu N, Muawad SA, Hughes CC. 2016. mTORC2 mediates CXCL12-induced angiogenesis. *Angiogenesis* **19**:359–371 DOI 10.1007/s10456-016-9509-6.